Comparative Medicine
Copyright 2005
by the American Association for Laboratory Animal Science

Vol 55, No 3
June 2005
Pages 236-243

Green Fluorescent Protein (GFP)-Expressing Tumor Model Derived from a Spontaneous Osteosarcoma in a Vascular Endothelial Growth Factor (VEGF)-GFP Transgenic Mouse

Peigen Huang, MD,* Trevor D. McKee, PhD, Rakesh K. Jain, PhD, and Dai Fukumura, MD, PhD

Vascular endothelial growth factor (VEGF) mediates tumor angiogenesis, growth, and metastasis. Murine models of metastatic tumors in which green fluorescent protein (GFP) expression is driven by the VEGF promoter can be imaged both intravitally and externally and thus offer many possibilities for real-time studies of tumor angiogenesis, metastasis, and treatment in vivo. In our defined-flora animal facility, an 11-month-old female transgenic mouse with a C3H background (*VEGF^P-GFP*/C3H) developed a spontaneous tumor that expressed GFP under the control of VEGF. Necropsy and histopathologic examination revealed an osteosarcoma with lung metastases. Fresh tumor fragments were transplanted successfully into other *VEGF^P-GFP*/C3H transgenic mice. During the first five generations, the tumor "take rate" was 100% (25 of 25 animals), with a latent period of 8 days and an average tumor volume of 1500 mm^3 at 36 days. Transplanted tumors have maintained their original histopathologic characteristics and metastatic behavior. In addition, the tumor grows in wild-type C3H mice with an 83% take rate (10 of 12 animals) and as monolayer cells in vitro. GFP was expressed strongly in tumor tissue, lung metastatic foci, and cultured tumor cells. Real-time growth of tumors grown in dorsal skin chambers in C3H mice could be visualized using GFP fluorescence. In addition, GFP fluorescence of metastatic lesions in lungs of C3H mice was clearly visible by multiphoton laser scanning microscopy. This in vitro and in vivo transplantable and metastatic osteosarcoma (Os-P0107) is an attractive model for further study of tumor pathophysiology and treatment efficiency affecting VEGF expression.

Animal models of metastatic tumors with genetically controlled green fluorescent protein (GFP) expression that can be imaged intravitally as well as externally offer many possibilities for real-time studies of tumor angiogenesis, metastasis, and experimental treatment studies in vivo (15). Most of these models have been developed using the cloned GFP gene from bioluminescent organisms and are then introduced into human and rodent tumor cell lines in vitro to stably express GFP in vivo after transplantation to rodent hosts (2, 6, 15, 25, 26). Here, we report a novel GFP tumor model that was directly derived from a spontaneous osteosarcoma in a *VEGF^P-GFP*/C3H transgenic mouse and showed high metastatic potential and strong GFP expression in tumor cells in vitro and in vivo. The reported frequency of occurrence of spontaneous osteosarcoma in mice is < 1% (11, 20). Spontaneous osteosarcoma in *VEGF^P-GFP*/C3H transgenic mice has not been described previously.

Materials and Methods

Animals and tumor transplantation. We used 6- to 10-week-old male and female homozygous *VEGF^P-GFP*/C3H transgenic and wild-type C3H mice. The mice were bred and maintained in our defined-flora animal facility (24). Under the facility microbiological monitoring program, all mice were sampled for aerobic bacteria before being weaned from the parent cages. Any mice exhibiting any aerobic bacterial growth were euthanized and removed from the colony. In addition, the sentinel mice in breed, stock, and experimental rooms were sent to an independent laboratory (Charles River Laboratory, Wilmington, Mass.) for complete diagnostic evaluations. Testing included bacteriology, infectious disease polymerase chain reaction (PCR) assays, parasitology, *Helicobacter* PCR tests, pathology, and serology examinations. All sentinel mice were screened for 18 murine viruses, all pathogenic aerobic bacteria, and parasites, including Sendai virus, mouse hepatitis virus, pneumonia virus of mice, minute virus of mice, mouse polio virus, reovirus type 3, *Mycoplasma pulmonis*, lymphocytic choriomeningitis virus, ectromelia virus, mouse pneumonitis virus, polyoma virus, mouse adenovirus FL/K87, epizootic diarrhea of infant mice virus, mouse cytomegalovirus, Hantaan virus, *Encephalitozoon cuniculi*, mouse thymic virus, mouse parvovirus, *Bordetella bronchoseptica*, *Corynebacterium kutscheri*, *Klebsiella oxytoca*, *K. pneumoniae*, *M. pulmonis*, *Pasteurella multocida*, *P. pneumotropica*, *Pasteurella* spp., *Pseudomonas aeruginosa*, *Pseudomonas* spp., *Staphylococcus aureus*, *Streptococcus pneumoniae*, *Salmonella* spp., *Citrobacter rodentium*, *Citrobacter* spp., *Helicobacter bilis*, *H. hepaticus*, *Helicobacter* spp., lice, mites, *Aspiculuris tetraptera*, *Syphacia muris*, *Sy. obvelata*, *Chilomastix* spp., *Entamoeba* spp., *Giardia* spp., *Hexamastix* spp., *Monocercomonides* spp., *Retortamonas* spp., *Spironucleus* spp., trichomonads, and protozoa. All test results were negative.

During the experimental period, all mice were housed in isola-

Received: 10/27/04. Revision requested: 12/7/04. Accepted: 2/8/05.
Department of Radiation Oncology, Edwin L. Steele Laboratory, Massachusetts General Hospital, Harvard Medical School, Boston, Massachusetts 02114.
**Corresponding author: Department of Radiation Oncology, Massachusetts General Hospital, 100 Blossom Street, Cox 7, Boston, Massachusetts 02114.*

tor cages, fed sterile laboratory pellets, and given acidified sterile water ad libitum. The spontaneous tumor that arose in a *VEGF^P-GFP*/C3H mouse was resected, cut into small pieces (approximately 2 mm in diameter), and transplanted subcutaneously (s.c.) into the flank of four 6-week-old female *VEGF^P-GFP*/C3H mice in order to obtain the first-generation isograft (F1). When F1 tumors reached approximately 1.5 cm in diameter, one of the isografts was excised and transplanted to the next set of five *VEGF^P-GFP*/C3H mice for F2 tumors. In each generation from F2 to F5, tumor tissue also was transplanted s.c. into three wild-type C3H mice for comparison. This tumor model, designated Os-P0107, has been serially passaged in vivo up to F8. All animal procedures were carried out following the *Public Health Service Policy on Humane Care of Laboratory Animals* (23) and approved by the Institution Animal Care and Use Committee at the Massachusetts General Hospital.

Histopathological analysis. Tissue specimens obtained from the spontaneous tumor, lungs, and tumor isografts were fixed in 10% neutral buffered formalin, embedded in paraffin, cut at 5-μm thickness, and stained with hematoxylin and eosin (H&E) for histological examination. Fresh tumor tissue also was fixed in 4% paraformaldehyde for 1 h at 4°C, washed in phosphate buffered saline (PBS), cryoprotected in 30% sucrose overnight, and frozen in OCT embedding compound (Sakura Finetek U.S.A. Inc. Torrance, Calif.). The OCT sections were observed under a fluorescence microscope (BX51, Olympus, Tokyo, Japan).

Cell culture. Fresh tumor tissue obtained from the F1 transplanted isograft was quickly cut into small pieces, cleared of necrotic tissue, washed twice in PBS, minced finely, and placed in a T-25 culture flask containing 5 ml of Dulbecco's modified Eagle's medium supplemented with 15% heat-inactivated fetal bovine serum and penicillin (100 units/ml) and streptomycin (100 mg/ml). The cells were incubated in 5% CO_2 at 37°C and passaged once or twice a week, so as to maintain an exponentially growing monolayer. The cells were detached using trypsin (0.05%) and versene (0.02%), when required. To determine GFP expression in vitro, cells were seeded on culture slides (BD Bioscience, Belford, Mass.). and allowed to grow overnight. Cells were fixed in 4% paraformaldehyde for 20 min, washed with PBS, and then stained with 1 μg/ml 4',6'-diamidino-2-phenylindole hydrochloride for 1 to 2 min. Slides were mounted in anti-fade solution and observed under the fluorescence microscope. Cells also were fixed in methanol for 15 min and stained with H&E for study of morphological characteristics.

Analysis of tumor growth and metastasis. The parameters of "take rate" (the number of animals in which the transplanted tissue implanted and grew divided by the number of animals transplanted), latent period (the number of days required for development of palpable s.c. tumors post-transplantation), and growth time (number of days required for the tumors to grow to 1500 ± 100 mm^3) were used to describe the growth characteristics of this tumor model. Two perpendicular diameters of the tumors were measured once per week with calipers. Tumor volume (V) was calculated as $V = a \times b^2/2$, where a and b are the long and short axes, respectively. For the purpose of determining metastatic potential, tumor chunks also were transplanted s.c. into the right hindleg of five *VEGF^P-GFP*/C3H and 12 C3H mice. When the tumors reached the volume of 500 ± 50 mm^3, the mice were anesthetized (90 mg/kg ketamine and 9 mg/kg xylazine s.c.), and the tumor-bearing legs were resected. The surgical procedure was described previously (10). The mice were euthanized 5 months after surgical removal of the primary tumor or when they became moribund, whichever came first. Gross autopsy and histopathological analyses were performed then.

Dorsal skinfold chamber. Dorsal skinfold chambers were implanted in C3H mice (n = 12) as described previously (19). A small piece (approximately 1 mm in diameter) of an F1 or F2 isograft was implanted at the center of the chamber. Observations were made 1, 2, and 3 weeks after tumor implantation. The animals were positioned in a polycarbonate tube (inner diameter, 25 mm), and the chamber was fixed on a specially designed microscope stage.

Intravital and multiphoton laser scanning microscopy. Tumor growth in the chamber was monitored by intravital microscopy (Axioplan, Zeiss, Oberkochen, Germany) (6, 7). A fluorescence filter set for fluorescein (Omega Optical, Brattleboro, Vt.) was used to visualize GFP fluorescence. Micrometastases of lungs were examined ex vivo by using multiphoton laser scanning microscopy (1, 22) at an excitation wavelength of 840 nm. The sample was placed under a 20 × 0.5 NA water immersion lens, and fluorescent light was collected with the use of GFP (535/40) and autofluorescence (450/100) filters.

Statistical analysis. Data are expressed as mean ± SD. Statistical differences between groups were determined by an unpaired Mann-Whitney U test. Statistical analysis was performed using StatView 4.51 software (Abacus Concepts Inc., London, United Kingdom). $P < 0.05$ was considered to be statistically significant.

Results

Spontaneous osteosarcoma with lung metastases. The spontaneous tumor arose as a solid mass on the back of an 11-month-old congenic *VEGF^P-GFP*/C3H female transgenic mouse in our breeding group. Our *VEGF^P-GFP* transgenic mice originally were developed using FVB mice (*VEGF^P-GFP*/FVB). Subsequently, *VEGF^P-GFP*/FVB mice were crossed with C3H mice for three generations, and then homozygous *VEGF^P-GFP*/C3H mice were maintained as an inbred line. The original tumor was found when it was approximately 1.5 cm in diameter in the central sacral region of the mouse. The body weight of the tumor-bearing host was 33 g. The mouse was euthanized and necropsied. A multicolored oval mass of 1.5 × 1.4 × 1.2 cm and an intact surface was revealed. The tumor was gritty, had attached to the sacrum, and had invaded the surrounding musculature. Lung metastases were found also. The metastatic foci were multiple white or gray nodules on the surface of the lungs. Microscopic examination revealed that the spontaneous tumor mainly was composed of osteoid, bony trabeculae resembling fibrosarcomatous tissue, and osteoclasts (Fig. 1A and B). The interlacing bundles of polygonal to spindle-shaped tumor cells were present in areas of the tissue that closely resembled fibrosarcoma. Tumor cells with round or oval nuclei were palisaded along the borders of osteoid and were punctuated by numerous giant cells with multiple nuclei, resembling osteoblasts (Fig. 1A through C). Many thin-walled blood vessels were present in the tumor stroma (Fig. 1B). The primary spontaneous tumor and its multiple metastatic foci in the lungs microscopically resembled each other closely. Tumor cells, osteoid, and bone formation similar to those of the primary tumor were found in the lung deposits (Fig. 1D). The pathohistological diagnosis was spontaneous osteosarcoma with multiple lung metastases.

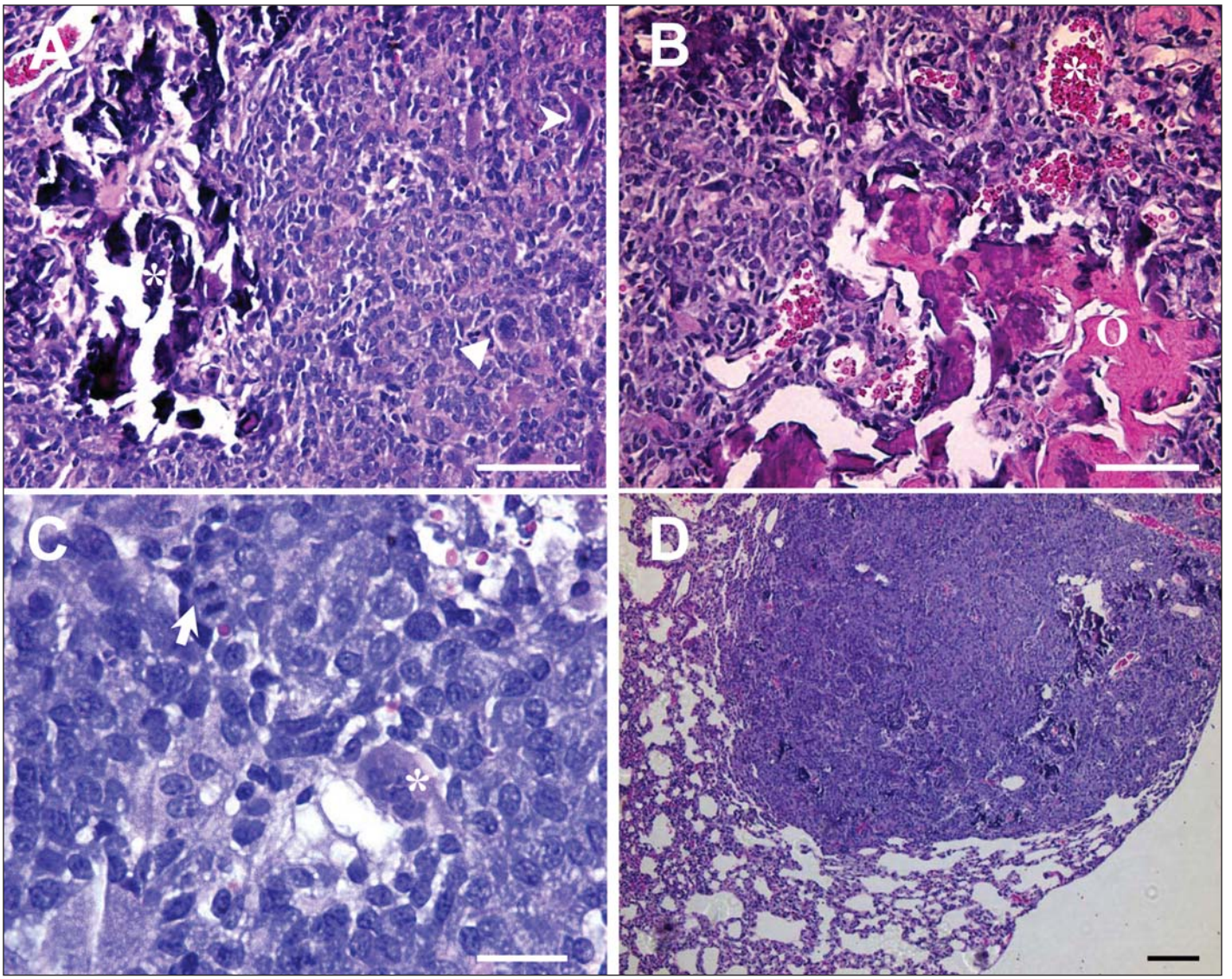

Figure 1. (A and B) Photomicrographs of the sections of the original spontaneous osteosarcoma in a *VEGF^{P}-GFP*/C3H transgenic mouse, showing the polygonal to spindle-shaped tumor cells, giant cells (A, arrows), trabeculae of osteoid (B, O), partial calcification (A, *), and many thin-walled (B, *) vessels in the tumor stroma. H&E stain; bar, 100 µm. (C) Higher magnification view of neoplastic cells with round or oval nuclei, a giant cell with multiple nuclei (*), and a mitotic figure (arrow). H&E stain; bar, 25 µm. (D) Photomicrograph of a section of the metastasis in lung, showing tumor cells and partially calcified osteoid similar to that in the primary tumor. H&E stain; bar, 100 µm.

High transplantability of the osteosarcoma isografts. This spontaneous osteosarcoma, Os-P0107, has been successfully transplanted and passaged serially in the subcutaneous tissue of homozygous *VEGF^{P}-GFP*/C3H transgenic mice with a 100% take rate; the tumor also is accepted by wild-type C3H mice with an 83% take rate and progressive growth behavior. Figure 2 gives the growth curves of tumors derived from F1 to F5 isografts in 25 *VEGF^{P}-GFP*/C3H mice (Fig. 2A) and of the F2 to F5 isografts in the 10 of the 12 C3H mice into which tumor was transplanted (Fig. 2B). Both curves show the latent period to the development of palpable tumor and the growth pattern at different passages in vivo; there is a tendency toward increased growth rate with in vivo passage. Table 1 shows the isotransplant take rate, latent period, and growth time of the isografts grown in *VEGF^{P}-GFP*/C3H and C3H mice. As shown in Table 1, the isografits grown in wild-type C3H mice exhibited lower take rates, longer latent periods and growth times in comparison to the tumors grown in *VEGFP-GFP*/C3H mice. However, only the difference in growth time achieved statistical significance (Mann-Whitney U test, $P = 0.02$).

The osteosarcoma is highly metastatic. Tumors were transplanted subcutaneously in the right hindlegs of five *VEGF^{P}-GFP*/C3H and 12 C3H mice and were allowed to reach 500 ± 50 mm^3. The primary tumors then were removed at 25.6 ± 3.3 (*VEGF^{P}-GFP*/C3H) and 26.0 ± 3.5 (C3H) days. Table 2 gives the number of days until necropsy, incidence of spontaneous metastasis, and site of metastasis for both types of recipient mice. All 17 mice developed lung metastases. In five of the mice, tumors metastasized to the inguinal or iliac lymph nodes. Skeletal metastases were found in two mice, in the humerus or a vertebra (Fig. 3A). Metastatic foci in the lungs (Fig. 3B), lymph nodes, and bones were identified macroscopically. Most of the metastatic foci were presented as white or gray nodules on the surface of

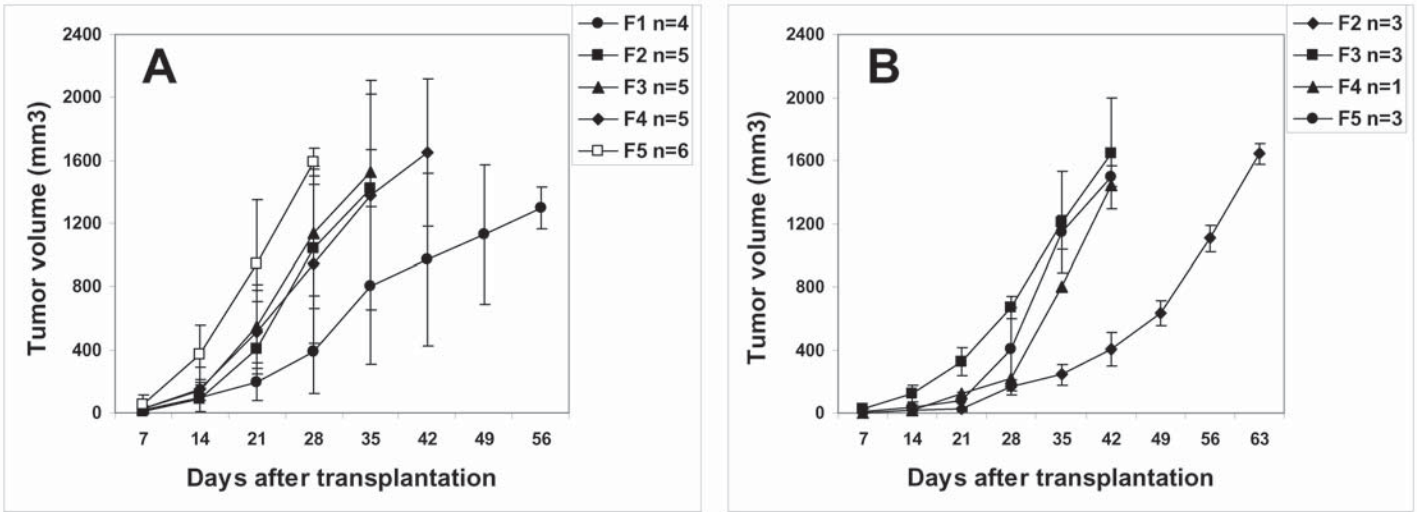

Figure 2. (A) Growth curves of tumors derived from F1 to F5 isografts in 25 homozygous *VEGF^P-GFP*/C3H mice. The data points are the mean tumor volume; bars indicate 1 SD. (B) F2 to F5 isografts in the 10 C3H mice in which transplantation of tumor tissue was successful. The data are the mean tumor volume; bars indicate 1 SD.

Table 1. Growth characteristics of Os-P0107 tumors in homozygous *VEGF^P-GFP*/C3H transgenic and wild-type C3H mice

Mice	Take rate	Latent period (days)	Growth time (days)[a]
VEGF^P-GFP/C3H	100% (25 of 25)	8.4 ± 6.2	36.2 ± 11.7
C3H	83% (10 of 12)	11.7 ± 6.4	46.9 ± 9.6

Data are given as mean ± 1 standard deviation.
[a]The growth time is the number of days needed for the tumor to reach 500 mm^3 and differs statistically (Mann-Whitney U test, $P = 0.02$) between the two strains of mice.

the lungs. Metastases in lymph nodes and bones caused their volumes to increase markedly with irregular shapes.

Metastases were confirmed histologically (Fig. 3C). All examined cases (n = 12) showed close morphological resemblance between the subcutaneous isografts and their metastatic colonies in distant organs. The results show that Os-P0107 isografts retained the high metastatic potential of the original spontaneous osteosarcoma. The isografts all expressed spontaneous metastases, not only in homozygous *VEGF^P-GFP*/C3H transgenic mice but also in wild-type C3H mice. The times until tumor removal and necropsy and characteristics of the metastases in these recipient mice were comparable.

Strong expression of GFP in tumor cells in vivo and in vitro. Tumor tissue from F2 and F5 isografts were examined using the fluorescence microscope immediately after sample collection, and all the tumor specimens were strongly fluorescent (Fig. 4A), showing stable GFP-expression in vivo during the tumor passages. Metastatic foci from the lung also were fluorescent (Fig. 3D).

A cell line was established from the F1 tumor tissue. The cells growing as monolayers were maintained and passaged in vitro. The morphology of the cultured Os-P0107 cells in the growth phase (Fig. 4B) revealed polygonal and spindle-shaped cells with round or oval nuclei and mitotic figures. The exponentially growing cells exhibited a strikingly bright GFP fluorescence (Fig. 4C), and more than half of the cells showed strong GFP expression at any given time (Fig. 4D).

Visualization of GFP-expressing tumor in dorsal skinfold chambers and of lung micrometastases. Figure 5A shows an intravital GFP fluorescent image of an Os-P0107 tumor grown in a dorsal skin chamber in a C3H mouse. The angiogenic blood vessels are shown as dark structures (negative contrast), whereas tumor cells exhibit bright GFP fluorescence. The GFP fluorescence is more intense in the region distant from the blood vessels.

Figure 5B shows a GFP fluorescence image of the excised lung of a C3H mouse with metastatic lesions. As a control, the autofluorescence image of the normal fresh lung tissue also was obtained (Fig. 5C). With multiphoton laser scanning microscopy, the GFP fluorescence of the metastatic foci is clearly visible, compared with the autofluorescence of normal lung tissue.

Discussion

We report a novel GFP expressing tumor model, Os-P0107, which was directly derived from a spontaneous osteosarcoma in a *VEGF^P-GFP*/C3H transgenic mouse and showed high transplantability, high metastatic potential, and strong GFP expression in tumor cells both in vitro and in vivo. Spontaneous osteosarcoma is rare in mice (3, 11, 20) and has not been described previously to occur in *VEGF^P-GFP*/C3H transgenic mice. However, we and others have reported cases of spontaneous osteosarcoma in SCID and C57BL/6 mice; these tumors commonly caused distant lung metastases (3, 11) and were transplantable (11).

The Os-P0107 tumor was transplanted successfully into *VEGF^P-GFP*/C3H transgenic mice and passaged serially in vivo with a 100% take rate, latent period of 8 days, and average tumor volume of 1500 mm^3 at 36 days during the first five generations. The tumor also was accepted by wild-type C3H mice with an 83% take rate and progressive growth behavior. The tumors grown in C3H mice exhibited latent periods and take rates comparable with those of isotransplants in *VEGF^P-GFP*/C3H transgenic mice. However, the growth time was significantly different between these recipient mice (Mann–Whitney U test, $P = 0.02$). The results suggest that a complete match of strain background between the primary spontaneous tumor and the recipient is required to obtain 100% tumor take and makes tumors grow faster. Nevertheless, tumors grow in both *VEGF^P-GFP*/C3H and C3H wild-type mice showed a tendency toward increased growth rate with in vivo passage. Research conducted in our laboratory

Table 2. Behavior of metastatic Os-*P0107* tumors in homozygous *VEGF^P-GFP*/C3H transgenic and wild-type C3H mice

Mice	Time until necropsy (days)	Incidence of metastasis	Sites of metastasis		
			Lung	Lymph node	Bone
VEGF^P-GFP/C3H (n = 5)	104.0 ± 19.2	100%	5	2	1
C3H (n = 12)	115.4 ± 25.6	100%	12	3	1

Data are given as mean ± 1 standard deviation.

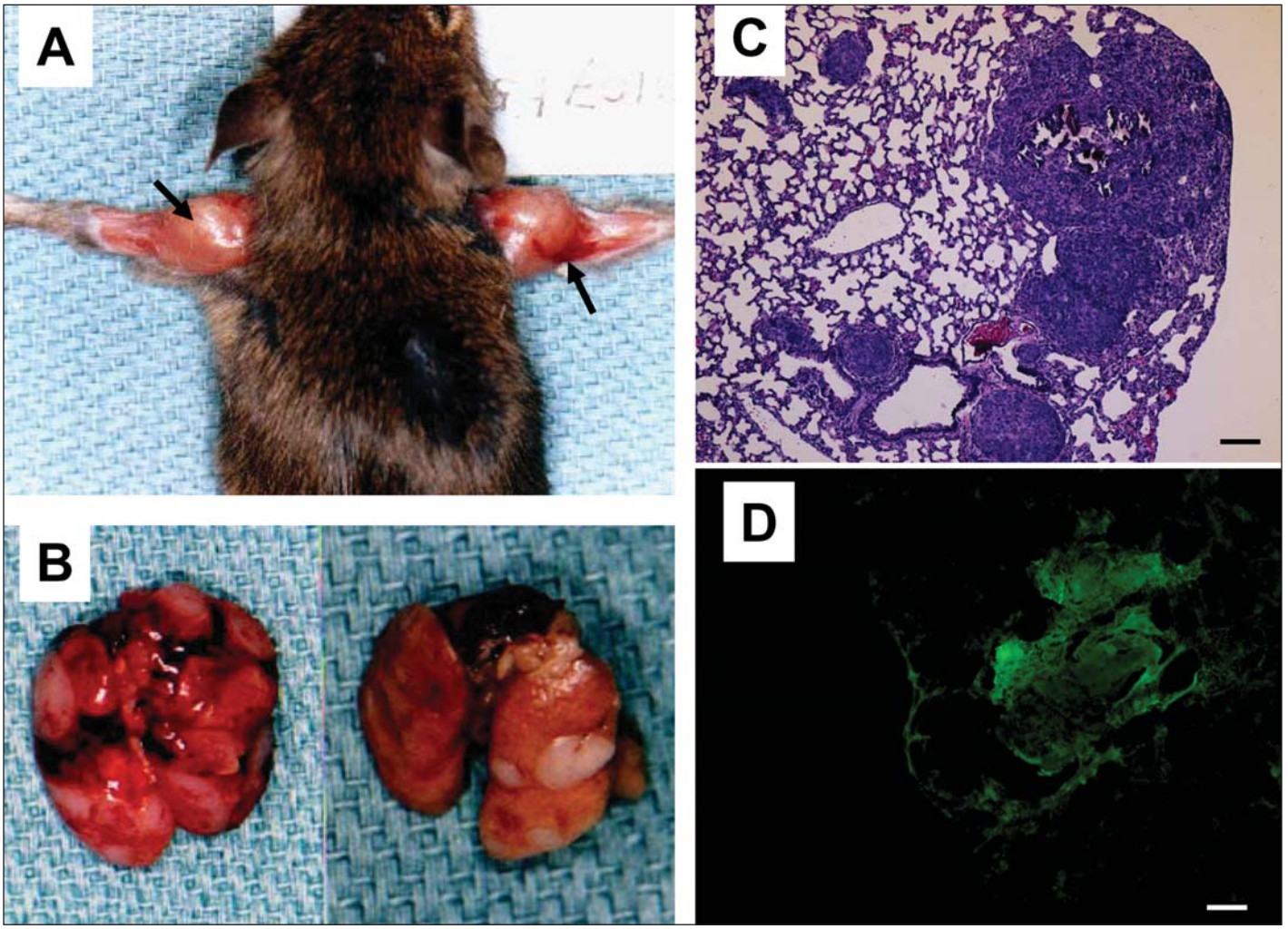

Figure 3. Photographs of Os-P0107 isografts metastases to humeri (A, arrows) and lungs (B). Lung metastases were confirmed histologically (C, H&E stain). (D) GFP fluorescent metastatic foci in lung specimens from a C3H mouse. Bar, 100 μm.

and others' (13, 21) indicates that serial in vivo passage leads to faster tumor growth in mice.

To test the metastatic characteristics of the Os-P0107 tumors transplanted in *VEGF^P-GFP*/C3H and C3H wild-type mice, we removed the primary isografts when the tumor volumes reached 500 mm^3 and then examined the mice at 5 months after the surgical removal of primary tumor or when the mice became moribund. Our results show all isografts fully expressed spontaneous metastases, not only in homozygous *VEGF^P-GFP*/C3H transgenic mice but also in wild-type C3H mice. Surgical removal of the primary s.c. tumor allows the host mouse to survive long enough to develop distant metastatic tumors (10, 12). This procedure is necessary because of the rapid growth of the primary tumor and the permitted tumor size limit. However, removal of the primary tumor may increase metastatic tumor growth if the primary tumors produce endogenous anti-angiogenic molecules (5).

We established not only a transplantable tumor line in vivo but also an Os-P0107 cell line in vitro. The cultured cells growing as monolayers have been maintained and passaged for more than 10 passages in vitro and show the morphological characteristics of osteosarcoma cells as well as strong GFP expression in more than half of the cells at any given time. Although the establishment of a new osteogenic cell line from a spontaneous mouse osteosarcoma has been described (16), we believe that ours is the first report of a tumor cell line derived from a spontaneous osteosarcoma in a *VEGF^P-GFP*/C3H transgenic mouse and that shows strong GFP expression.

Real-time tumor angiogenesis, tumor growth, and tumor cell migration (not shown) can been visualized by following the GFP fluorescence of Os-P0107 tumors grown in dorsal skin chambers

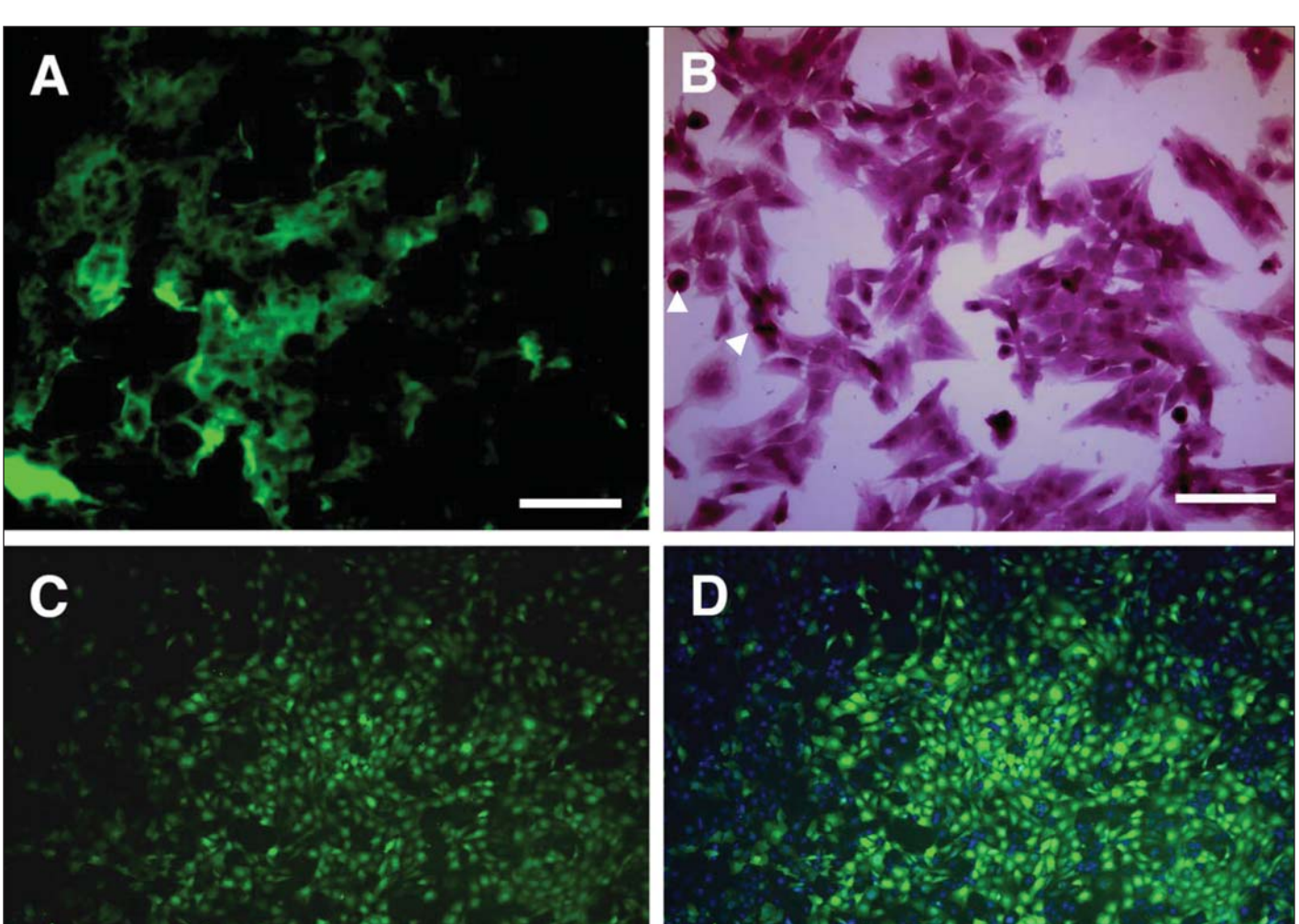

Figure 4. (A) Fresh tissue from the isotransplanted tumor with intense fluorescence of GFP. (B) Morphological features of Os-P0107 in growth phase (2 days of in vitro culture), showing the polygonal and spindle-shaped cells with round or oval nuclei and mitotic figures (arrows). H&E stain. (C) Exponentially growing tumor cells had marked GFP fluorescence. (D) DAPI staining for cell nuclei. Bar, 100 μm.

of wild-type C3H mice. Angiogenic blood vessels presented as dark structures, whereas tumor cells exhibited bright GFP fluorescence, when we used intravital microscopy to monitor tumor growth in the chamber. The GFP fluorescence was more intense in regions distant from the blood vessels. We think that hypoxia or acidic pH may induce VEGF promoter activity in these cells (8), presumably because of the spatial gradient of tissue oxygen and pH from the blood vessels (9). In addition, multiphoton laser scanning microscopy easily revealed the GFP fluorescence of micrometastatic Os-P0107 lesions in the lungs of C3H mice.

In conclusion, our results show that Os-P0107 is a novel GFP-expressing tumor model that was derived from a spontaneous osteosarcoma in a VEGF-GFP transgenic mouse. This tumor is highly metastatic and strongly expresses GFP under the control of the VEGF promoter in tumor cells both in vitro and in vivo. The Os-P0107 GFP-expressing tumor can be visualized in situ as well as ex vivo and thus is useful for real-time studies of tumor angiogenesis, metastasis, and preclinical treatments that affect VEGF expression. This model is clinically relevant and timely because VEGF expression by osteosarcomas has been associated with pulmonary metastasis and poor prognosis (17); in addition, serum VEGF can be used to identify early recurrence of osteosarcoma in clinical patients (18). Various therapeutic strategies to target VEGF signaling are being investigated extensively in preclinical and clinical settings (4, 14).

Acknowledgments

This study was supported by grants R24-CA-85140 and P01-CA-80124 from the National Institutes of Health. We thank Sylvie Roberge, Julia Kahn, Russell Delgiacco, and Chenmei Luo for excellent technical support and Leo Gerweck, Ricky Tong, and Robert Sedlacek for helpful discussions.

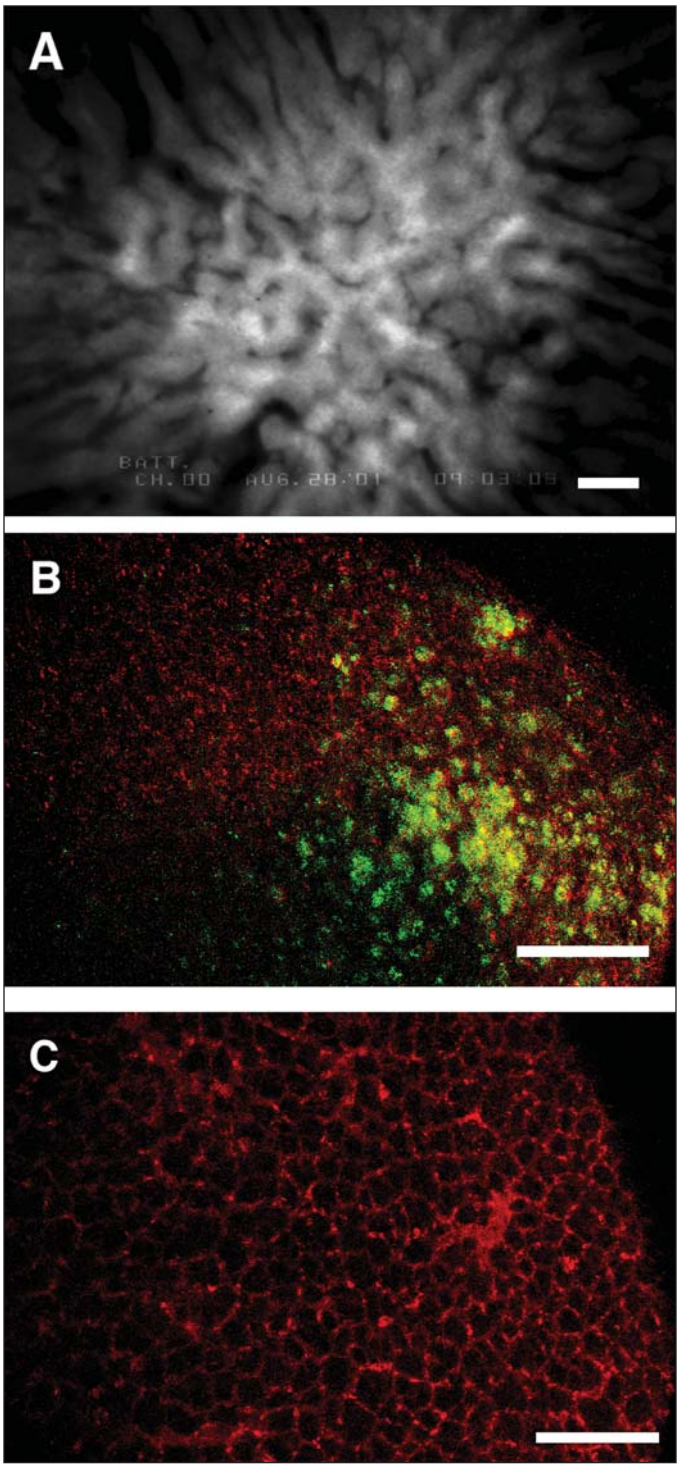

Figure 5. (A) GFP fluorescence image obtained by intravital microscopy of Os-P0107 tumor grown in the dorsal skin chamber of a C3H mouse. Blood vessels are shown as dark structure (negative contrast). VEGF-GFP fluorescence is more intense distant from blood vessels (hypoxic region of tumor). Bar, 100 µm. (B) GFP fluorescence image obtained by multiphoton laser scanning microscopy of metastatic lesions in fresh lung sample from a C3H mouse. Bar, 100 µm. (C) Autofluorescence imaging of normal lung tissue of C3H mouse as control. Bar, 100 µm.

References

1. **Brown, E. B., R. B. Campbell, Y. Tsuzuki, L. Xu, P. Carmeliet, D. Fukumura, and R. K. Jain.** 2001. In vivo measurement of gene expression, angiogenesis and physiological function in tumors using multiphoton laser scanning microscopy. Nat. Med. **7:**864-868.
2. **Chishima, T., Y. Miyagi, X. Wang, H. Yamaoka, H. Shimada, A. R. Moossa, and R. M. Hoffman.** 1997. Cancer invasion and micrometastasis visualized in live tissue by green fluorescent protein expression. Cancer Res. **57:**2042-2047.
3. **Cockman-Thomas, R. A., D. G. Dunn, W. Innskeep, II, W. L. Mondy, and J. R. Swearengen.** 1994. Spontaneous osteosarcom in a C57BL/6J mouse. Lab. Anim. Sci. **44:**531-533.
4. **Ferrara, N.** 2002. VEGF and the quest for tumor angiogenesis factors. Nat. Rev. Cancer **2:**795-803.
5. **Folkman, J. and R. Kalluri.** 2003. Tumor angiogenesis, p. 161-194. *In* D. W. Kufe, R. E. Pollock, R. R. Weichselbaum, R. C. Bast, Jr., J. F. Holland, and E. Frei, III (ed.), Cancer medicine, 6th ed. B. C. Decker, Hamilton, Ontario, Canada.
6. **Fukumura, D., R. Xavier, T. Sugiura, Y. Chen, E. Park, N. Lu, M. Selig, G. Nielsen, T. Takir, R. K. Jain, and B. Seed.** 1998. Tumor induction of VEGF promoter activity in stromal cells. Cell **94:**715-725.
7. **Fukumura, D., L. Xu, Y. Chen, T. Gohongi, B. Seed, and R. K. Jain.** 2001. Hypoxia and acidosis independently up-regulate vascular endothelial growth factor transcription in brain tumors in vivo. Cancer Res. **61:**6020-6024.
8. **Fukumura, D., F. Yuan, M. Endo, and R. K. Jain.** 1997. Role of nitric oxide in tumor microcirculation: blood flow, vascular permeability, and leukocyte-endothelial interactions. Am. J. Pathol. **150:**713-715.
9. **Helmlinger, G., F. Yung, M. Dellian, and R. K. Jain.** 1997. Interstitial pH and pO_2 gradients in solid tumors in vivo: high-resolution measurements reveal a lack of correlation. Nat. Med. **3:**177-182.
10. **Huang, P., A. Allam, A. Taghian, J. Freeman, M. Duffy, and H. D. Suit.** 1995. Growth and metastatic behavior of five human glioblastomas compared with nine other histological types of human tumor xenografts in SCID mice. J. Neurosurg. **83:**308-315.
11. **Huang, P. and H. D. Suit.** 1996. Spontaneous osteosarcoma in a severe combined immunodeficient (SCID/Sed) mouse. Contemp. Top. Lab. Anim. Sci. **35(6):**75-77.
12. **Huang, P., A. Taghian, D. W. Hsu, L. A. Perez, A. Allam, M. Duffy, A. DaCosta, and H. D. Suit.** 1996. Spontaneous metastasis, proliferation characteristics and radiation sensitivity of fractionated irradiation recurrent and unirradiated human xenografts. Radiother. Oncol. **41:**73-81.
13. **Izumi, Y., E. diTomaso, A. Hooper, P. Huang, J. Huber, D. J. Hicklin, D. Fukumura, R. K. Jain, and H. D. Suit.** 2003. Responses to anti-angiogenesis treatment of spontaneous autochthonous tumors and their isografts. Cancer Res. **63:**747-751.
14. **Jain, R. K.** 2005. Normalization of tumor vasculature: an emerging concept in antiangiogenic therapy. Science **307:**58-62
15. **Jain, R. K., L. L. Munn, and D. Fukumura.** 2002. Dissecting tumors using intravital microscopy. Nat. Rev. Cancer **2:**266-276.
16. **Joliat, M. J., S. Umeda, B. L. Lyons, M. A. Lynes, and L. D. Shultz.** 2002. Establishment and characterization of a new osteogenic cell line (MOS-J) from a spontaneous C57BL/6J mouse osteosarcoma. In Vivo **16:**223-228.
17. **Kaya, M., T. Wada, T. Akatsuka, S. Kawaguchi, S. Nagoya, M. Shindoh, F. Higashino, F. Mezawa, F. Okada, and S. Ishii.** 2000. Vascular endothelial growth factor expression in untreated osteosarcoma is predictive of pulmonary metastasis and poor prognosis. Clin. Cancer Res. **6:**572-577.
18. **Kaya, M., T. Wada, S. Kawaguchi, S. Nagoya, T. Yamashita, Y. Abe, H. Hiraga, K. Isu, M. Shindoh, F. Higashino, F. Okada, M. Tada, S. Yamawaki, and S. Ishii.** 2002. Increased pre-therapeutic serum vascular endothelial growth factor in patients with early clinical relapse of osteosarcoma. Br. J. Cancer **86:**864-869.

19. **Leunig, M., F. Yuan, M. D. Menger, Y. Boucher, A. E. Goetz, K. Messmer, and R. K. Jain.** 1992. Angiogenesis, microvascular architecture, microhemodynamics, and interstitial fluid pressure during early growth of human adenocarcinoma LS174T in SCID mice. Cancer Res. **52:**6553-6560.
20. **Lombard, L. S.** 1982. Neoplasms of musculoskeletal system, p. 501-511. *In* H. L. Foster, J. D. Small, and J. G. Fox (ed.), The mouse in biomedical research, vol. IV: experimental biology and oncology. Academic Press, Inc., New York.
21. **McCredie, J. A., W. R. Inch, and R. M. Sutherland.** 1971. Differences in growth and morphology between the spontaneous C3H mammary carcinoma and its syngeneic transplants. Cancer **27:**635-642.
22. **Padera, T. P., B. R. Stoll, P. T. C. So, and R. K. Jain.** 2002. Conventional and high-speed intravital multiphoton laser scanning microscopy of microvasculature, lymphatics, and leukocyte-endothelial interactions. Mol. Imaging **1:**9-15.
23. **Public Health Service.** 1996. Public Health Service Policy on Humane Care and Use of Laboratory Animals. Washington, D.C.: U.S. Department of Health and Human Services, 28 pp. [PL 99-158, Health Research Extension Act, 1985].
24. **Sedlacek, R., R. P. Orcutt, H. D. Suit, and E. F. Rose.** 1981. A flexible barrier at cage level for existing colonies: production and maintenance of a limited stable anaerobic flora in a closed inbred mouse colony, p. 65-69. *In* S. Sazaki, A. Ozawa, and K. Hashimoto (ed.), Recent advances in germfree research. Tokai University Press, Tokyo.
25. **Yang, M., E. Baranov, X-M. Li, J. W. Wang, P. Jiang, L. Li, A. R. Moossa, S. Penman, and R. M. Hoffman.** 2001. Whole-body and intravital optical imaging of angiogenesis in orthotopically implanted tumors. Proc. Natl. Acad. Sci. USA **98:**2616-2621.
26. **Yang, M., P. Jiang, F-X. Sun, S. Hasegawa, E. Baranov, T. Chishima, H. Shimada, A. R. Moossa, and R. M. Hoffman.** 1999. A fluorescent orthotopic bone metastasis model of human prostate cancer. Cancer Res. **59:**781-786.